Flexural Behavior of Sprayed Lightweight Composite Mortar-original Bamboo Composite Beams: Experimental Study

Li-min Tian,[a,b,*] Yue-feng Kou,[a] and Ji-ping Hao [a]

To study the flexural behavior of a composite beam, original single and double bamboo beams (SBBs and DBBs, respectively) and sprayed lightweight composite mortar-original bamboo composite beams (SCBs and DCBs) were designed and subjected to a four-point bending test based on the moisture content of the original bamboo. The failure modes, bearing capacity, and initial flexural rigidity of all of the beams were analyzed. Also, the strengthening effect of the lightweight composite mortar on the flexural behavior was studied. The results showed that a higher moisture content in the bamboo degraded the anti-slip property of the bond interface between the lightweight composite mortar and bamboo. The moisture content of the bamboo should be kept at approximately 20% before spraying. The initial flexural rigidity and bearing capacity of the DBBs were approximately 2.5 times and twice that of the SBBs, respectively. The initial flexural rigidities of the SCBs and DCBs were approximately 3.8 and 5.7 times that of the SBBs and DBBs, respectively. The ultimate load bearing capacity of the composite beams was approximately 1.5 times that of the original bamboo beams. It was shown that the lightweight composite mortar had a remarkable strengthening effect on the flexural behavior of the original bamboo.

Keywords: Sprayed lightweight composite mortar; Original bamboo beam; Composite beam; Critical bamboo moisture content; Initial flexural rigidity; Bearing capacity

Contact information: a: School of Civil Engineering, Xi'an University of Architecture and Technology, Xi'an 710055; b: China Key Laboratory of Green Building in Western China, Xi'an 710055, China;
** Corresponding author: tianlimin@xauat.edu.cn*

INTRODUCTION

Bamboo is a high-quality material that is light, strong, and grows rapidly. It is a renewable and environmentally friendly biomass building material that is easy to obtain (van der Lugt *et al*. 2006; Nurdiah 2016). Many scholars have performed research that has promoted the many applications of bamboo in building structures (Yang *et al*. 2014; Askarinejad *et al*. 2015; Dixon *et al*. 2015). Many studies have examined the mechanical properties of bamboo by using small specimens (Lo *et al*. 2004; Ray *et al*. 2005; Tan *et al*. 2011). Such studies have considered the effects of the bamboo species, bamboo joint, loading direction, and humidity to determine the mechanical properties, such as the traditional tension, compression, and bending performances along the rift grain and cross grain, creep resistance, and anisotropy (Xiao *et al*. 2013; Dixon and Gibson 2014; Chen *at al*. 2015). However, full culm bamboo is typically used to construct rural low-rise houses and temporary structures, such as scaffolding and pavilions (Chung and Yu 2002; Kaminski 2013; Nurmadina *et al*. 2017). This is because the irregular geometry of bamboo causes problems in the building form and component connection, and traditional bamboo

buildings perform poorly in terms of fire resistance, heat insulation, and sound insulation. It is also difficult to meet comfort requirements when using bamboo in buildings.

Bamboo composites, such as bamboo scrimber and laminated bamboo, have become well-known because of their standardized shape and consistent material properties (Sharma *et al*. 2015). Li *et al*. (2016) tested the mechanical properties of laminated bamboo lumber (LBL) columns under radial eccentric compression to examine the failure modes by considering their eccentricities. Sinha *et al*. (2014) examined the structural performance of LBL and bamboo glulam beams (BGBs). The interlaminar shear of the LBL comprising the BGBs restricted the bending strength of the BGBs. To improve the load-carrying and spanning capacities of a structural member made of bamboo composites, some scholars have changed its section form or reinforced it with a fiber-reinforced polymer (FRP). Huang *et al*. (2016) studied a hollow deck made of a laminated bamboo composite with a good bearing capacity, which was suitable for use as flooring. Wei *et al*. (2017) investigated the flexural performance of bamboo scrimber beams strengthened with FRP composite sheets. Their experimental results demonstrated that the flexural load-carrying capacity and rigidity were effectively improved by the FRP composite sheets. However, most of such research has focused on processed bamboo (*e.g.*, bamboo slices and bundles), which does not have a good cylindrical bamboo structure. Additionally, processing bamboo inevitably uses adhesives, pressure, and other processes that consume energy and emit pollution.

To completely exploit the natural advantages of bamboo and overcome its deficiencies, Tian *et al*. (2018) proposed a sprayed lightweight composite mortar-original bamboo composite structure system, which had a good load bearing capacity, heat insulation, and fire resistance, for use in multilayer structures (Fig. 1).

Fig. 1. Process of spraying

When the construction technology of spraying is adopted to form a composite structure, it changes the dry/wet environment around the original bamboo. As such, the mechanical performance of the composite structure depends upon the bonding of the sprayed lightweight composite mortar and original bamboo. After spraying, the bamboo absorbs water from the sprayed lightweight composite mortar and starts to swell. However, during the curing process, the bamboo begins to lose water and shrinks. Therefore, during construction and curing, the size of the bamboo changes; this directly affects the bonding of the bamboo and sprayed lightweight composite mortar, which influences the mechanical performance of the composite structure.

This paper presented an experimental study on the anti-slip behavior of a sprayed lightweight composite mortar-original bamboo interface based on the bamboo moisture content to determine the critical bamboo moisture content for different bamboo diameters after spraying. In this study, composite beams were then formed by spraying the lightweight composite mortar on the surface of the original bamboo beam with this critical bamboo moisture content. The flexural behavior of the composite beams was examined, and the results of the composite beams were compared with those of the original bamboo beams. These results can provide a basis for engineering applications and theoretical analysis of composite beams.

EXPERIMENTAL

Materials

Bamboo

The Moso bamboo used in the experiment was four years old and from Zhejiang Province, China. A series of mechanical tests that analyzed the tensile strength along the rift grain, compressive strength along the rift grain, and Young's modulus along the rift grain were performed in accordance with the international standard for determining the physical and mechanical properties of bamboo (ISO 22157-1:2004 2004). The geometric characteristics of the specimens are shown in Fig. 2, and the properties are presented in Table 1.

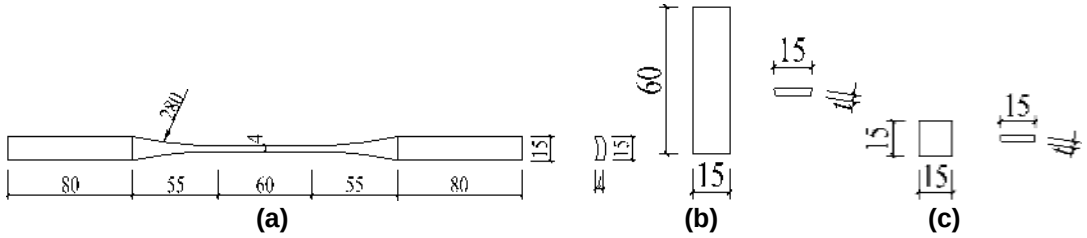

Fig. 2. Geometric characteristics of the specimens: (a) tensile strength and tensile Young's modulus; (b) compressive Young's modulus; and (c) compressive strength

Table 1. Properties of the Bamboo

$f_{b,t}$ (MPa)	$f_{b,c}$ (MPa)	$E_{b,t}$ (GPa)	$E_{b,c}$ (GPa)
193.2	66.3	12.9	11.9

Note: $f_{b,t}$ - Tensile strength; $f_{b,c}$ - Compressive strength; $E_{b,t}$ - Tensile Young's modulus; and $E_{b,c}$ - Compressive Young's modulus

When bamboo (shown in Fig. 3a) is pulled, a transverse crack is first formed on the inner side of the bamboo, and it rapidly expands in the longitudinal direction. Then, the fibers rupture and finally, tearing occurs. The section becomes uneven and broom-like (Fig. 3b). In contrast, when bamboo is compressed (Fig. 3c), because the vascular bundle distributed on the inner side is sparse, the fiber gets crushed and then gradually buckles from the inside out. Finally, the fiber folds and a staggered layer is formed (Fig. 3d).

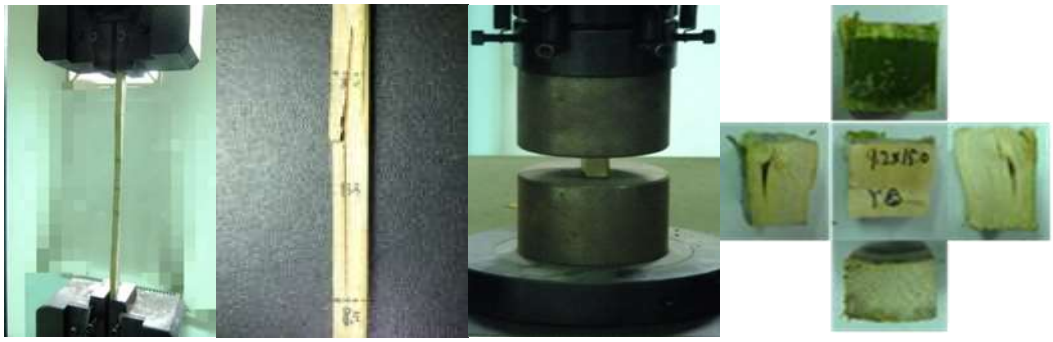

Fig. 3. Failure modes of the bamboo: (a) tensile specimen before breaking; (b) tensile specimen after breaking; (c) compressive specimen before breaking; and (d) compressive specimen after breaking

Sprayed lightweight composite mortar and cement mortar

The sprayed lightweight composite mortar is mainly composed of a combination of a gypsum-based mortar, polystyrene particles, and mineral adhesives (Liu *et al*. 2016). It was coated on the surface of a bamboo skeleton. The gypsum-based mortar can easily degrade after being discarded, and the polystyrene particles can reduce the self-weight of the lightweight composite mortar effectively. The mineral adhesives can change the rate of condensation of the lightweight composite mortar and improve its mechanical properties. After being sprayed, the lightweight composite mortar hardens rapidly and develops substantial strength and ideal thermal, acoustic, and fire resistance properties. The lightweight composite mortar not only leads to a low carbon footprint, but also remarkably improves living standards.

In this study, the mechanical properties of the sprayed lightweight composite mortar and cement mortar were measured with 100-mm × 100-mm × 300-mm prismatic test blocks (Fig. 4), and the results are presented in Table 2.

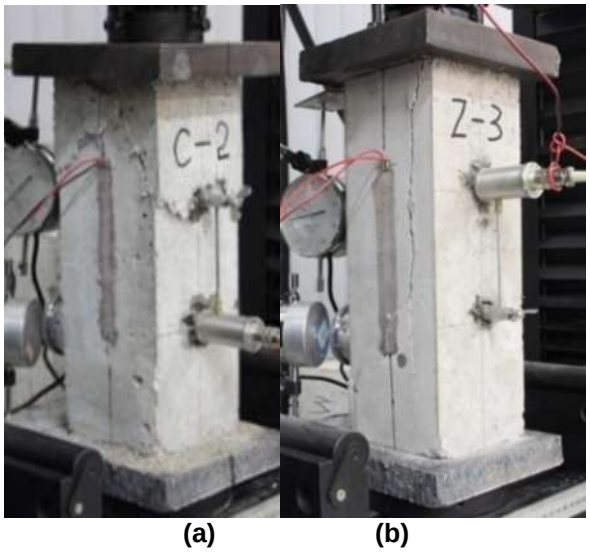

Fig. 4. Failure modes of the (a) sprayed lightweight composite mortar and (b) cement mortar

Table 2. Properties of the Sprayed Lightweight Composite Mortar and Cement Mortar

Specimen	Density (kg/m^3)	Compressive Strength (MPa)	Young's Modulus (GPa)
Sprayed Lightweight Composite Mortar	800.0	2.7	2.3
Cement Mortar	1845.8	12.8	10.1

Diameter Variation in the Bamboo after Spraying

A mechanical measurement method was used to test the diameter variation (DV). The tests were divided into two groups: S1 and S2. Each group had three specimens. The S1 and S2 specimens had bamboo moisture contents of 15% to 25% and 35% to 45%, respectively, when sprayed. For each specimen, three bamboo section pieces with a diameter of 100 mm were selected. The bamboo surface was sprayed with a 30-mm-thick layer of the lightweight composite mortar. In the second section, a measurement groove was set at the mid-length. The bamboo and lightweight composite mortar exposed by the measurement groove were waterproofed to ensure that the water exchange between the specimen and outside only occurred along the transverse direction. In the groove, four dividing points along the toroidal direction of the bamboo were set as measurement points 1 to 4, and a micrometer with a precision of 0.01 mm was used to periodically measure the bamboo diameters $D_{1\text{-}2}$ and $D_{3\text{-}4}$ between points 1 and 2 and points 3 and 4, respectively. Figure 5 shows the design and arrangement of the measurement points for each specimen. The specimens were sprayed on 26 July 2017 and cured under ordinary outdoor conditions, while avoiding direct sunlight. Figure 6 shows the environmental temperature and humidity variation with time.

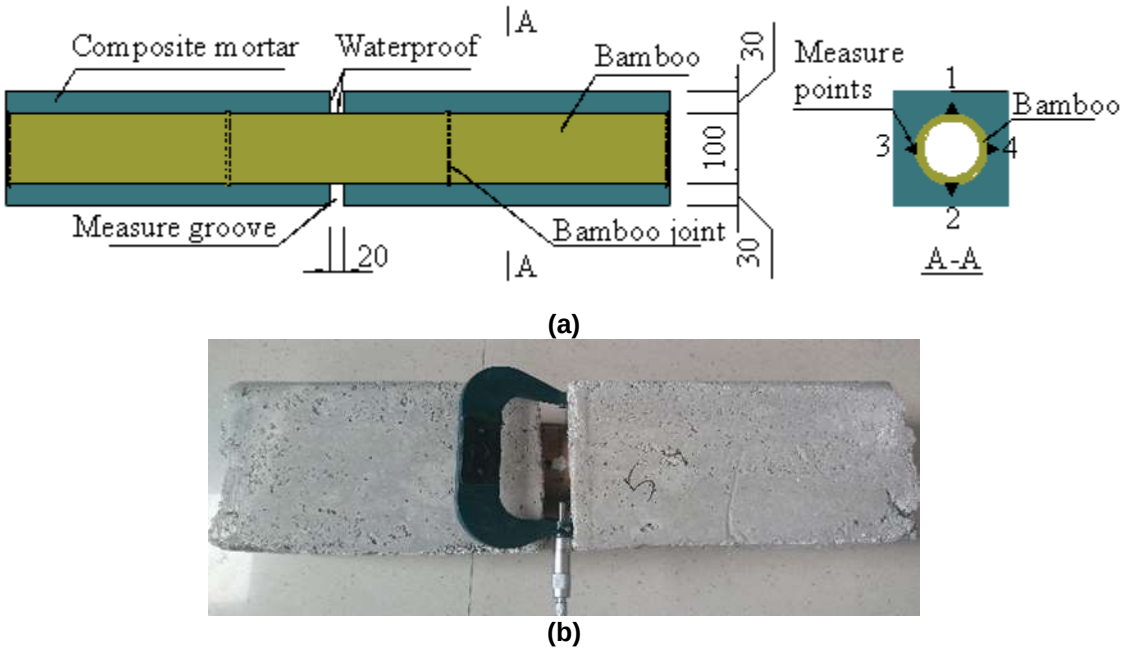

Fig. 5. Specimen design and arrangement of the measurement points: (a) design details (in mm); and (b) actual specimen for measurement

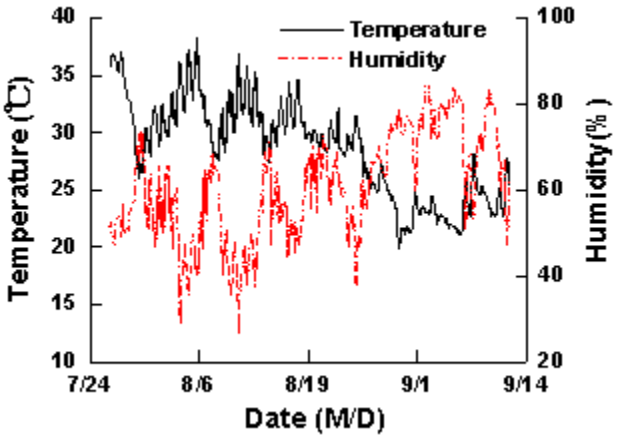

Fig. 6. Environmental temperature and humidity variation

Based on the measurement results, the following equation was used to calculate the percentage change (η, %) for the bamboo diameter:

$$\eta = \frac{(D_{1\text{-}2}+D_{3\text{-}4})_i - (D_{1\text{-}2}+D_{3\text{-}4})_0}{(D_{1\text{-}2}+D_{3\text{-}4})_0} \quad (1)$$

where i represents the days after spraying and 0 denotes the day before spraying.

Effect of the Bamboo Moisture Content on the Bond Behavior

Test specimens of the bamboo moisture content

Because the average air-dry moisture content (MC) of the bamboo was 18% during the experiment, a moisture content of 15% to 25% was taken as the starting interval, and the step length was set to 20%. The specimens were divided into three groups according to the moisture content of the bamboo when they were sprayed: A (55% to 65%), B (35% to 45%), and C (15% to 25%). The bamboo diameter was 100 mm, and the thickness of the lightweight composite mortar around the bamboo was 30 mm. To avoid effects from the bamboo joints, the specimens were designed without them at an embedment depth of 150 mm, and the distance between the end face of the lightweight composite mortar and bamboo joint was less than 20 mm. Figure 7 shows the details of the test specimens.

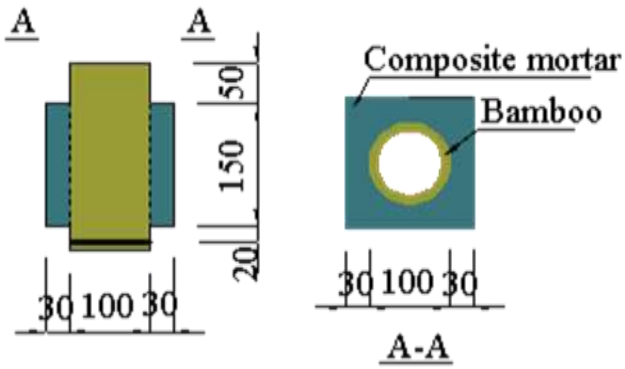

Fig. 7. Details of the moisture content specimens (in mm)

Testing methodology of the bamboo moisture content

The push-out test methodology was based on the experimental studies on the bond slip behavior between the steel section and concrete. A base was designed that operated with an electronic universal testing machine (DDL-20, Sinotest Equipment Co., Ltd., Changchun, China). The top of the base had a circular hole through which the bamboo could pass, but the lightweight composite mortar could not. The loading rate was 3 mm/min. Figure 8 shows a specimen and the test set-up. The measured average bamboo moisture contents of Groups A, B, and C were 60.8%, 40.2%, and 20.7%, respectively.

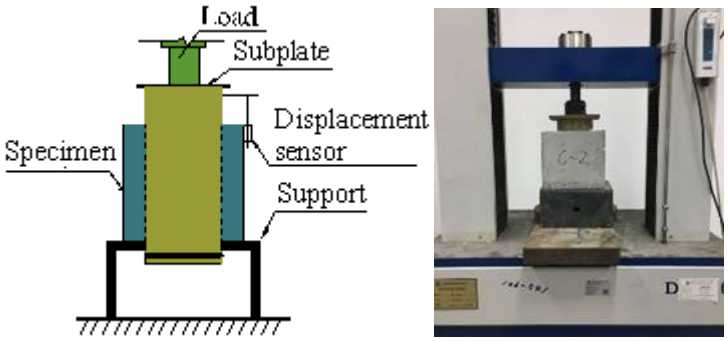

Fig. 8. Push-out test set-up

Analysis of the Flexural Behavior

Test specimens of the beams

The beams were divided into two groups based on the requirement of spraying the lightweight composite mortar. The first group contained original bamboo beams, including single original bamboo beams (SBBs) and double original bamboo beams (DBBs). The second group contained sprayed composite mortar-original bamboo composite beams, including single bamboo composite beams (SCBs) and double bamboo composite beams (DCBs). Among these beams, the DBBs and DCBs were the basic test specimens, each composed of two pieces, and the rest were composed of single pieces.

The length of the beams was 3000 mm, and the diameter and thickness of the bamboo in the mid-span were approximately 100 mm and 8 mm, respectively. The average moisture content of the original bamboo was approximately 20%. The original bamboos in the DBBs were connected by Φ10 bolts at three equidistant points and lashed with a 35-mm-wide steel belt in the middle of the adjacent bolts. The SCBs and DCBs were manufactured by spraying a 30-mm-thick lightweight composite mortar on the SBBs and DBBs, and then laying a wire mesh (8 mm × 8 mm × 0.6 mm) and plastering with a 10-mm-thick mortar layer. The properties of the beams are listed in Table 3.

Table 3. Properties of the Beams

Item	Component	Width (mm)	Height (mm)	Length (mm)
SBB	Single bamboo	100	100	3000
DBB-1	Two bamboos	100	200	
DBB-2				
SCB	Single bamboo + lightweight composite mortar + cement mortar	180	180	
DCB-1	Double bamboos + lightweight composite mortar + cement mortar	180	280	
DCB-2				

The geometric characteristics of the specimens are shown in Figs. 9 and 10. The manufacturing process of the composite beams is shown in Fig. 11.

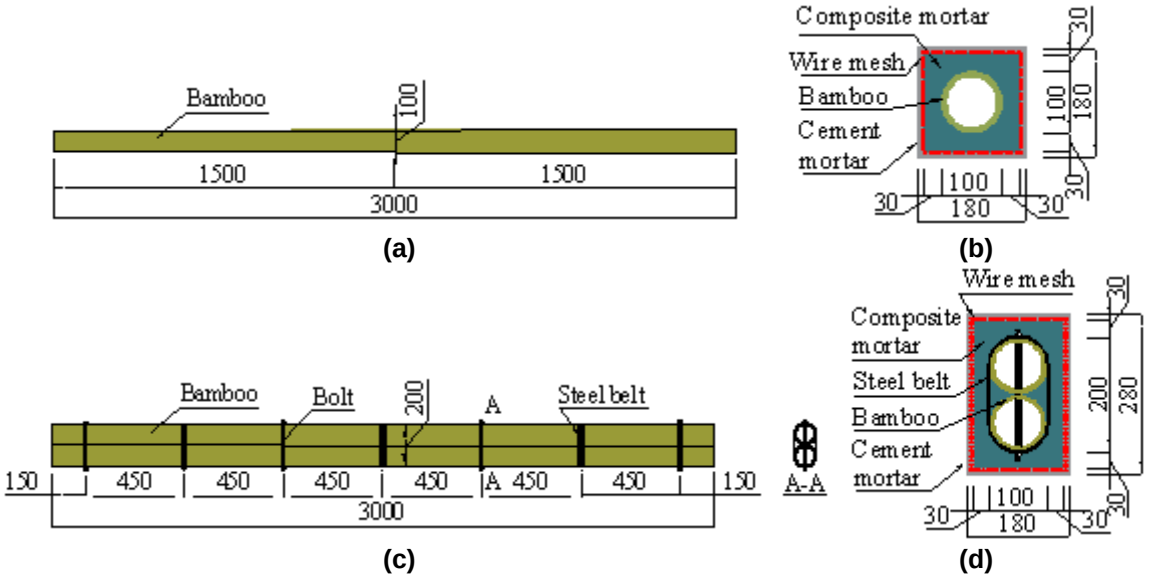

Fig. 9. Design details of the beams (in mm): (a) SBB, (b) SCB, (c) DBB, and (d) DCB

(a)

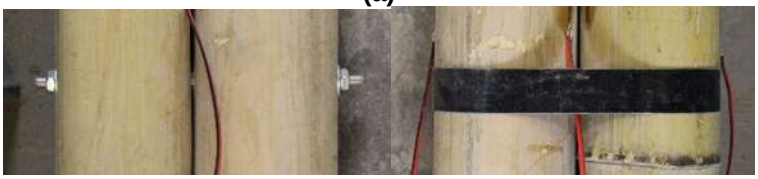

(c) (d)

Fig. 10. Actual connection in the bamboos: (a) DBB, (b) bolt, and (c) steel belt

Fig. 11. Manufacturing process of the composite beams

Test set-up of the beams

A hydraulic jack was used to apply a load at the three equidistant points of the beams *via* a distributive beam. It should be noted that the arc-shaped wood spacers in the SBBs and DBBs, which fit the outer diameter of the original bamboo, were arranged at the loading points and supports to ensure that the original bamboo remained fixed in their positions and did not fracture prematurely. Simultaneously, to prevent the SBBs and DBBs from overturning or out-of-plane flexural buckling, two pairs of lateral braces were arranged on both sides of the specimens. The set-up of the beams (take DBB as an example) is presented in Fig. 12.

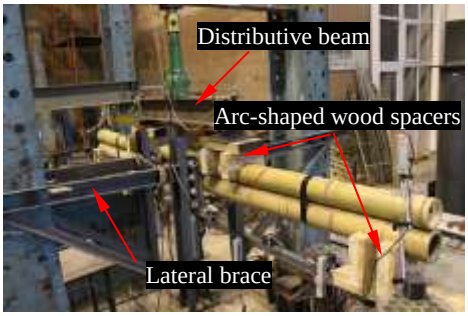

Fig. 12. Test set-up of the beams

The method of grading loading was adopted. Initially, according to the load control, the load for each stage was increased by 2 kN. When the beams yielded, the control was changed to the displacement control, and the displacement for each stage was increased by 5 mm until the beams were destroyed. To obtain the deflection and strain of the specimens, a total of five displacement sensors (D1 to D5) were arranged along the length of the beams. Strain gauges were placed on the upper and lower edges of the original bamboo in the middle of the beams. Test data was collected by a TDS-530 static data acquisition instrument (Tokyo Measuring Instruments Laboratory Co., Ltd., Japan). The arrangement of each measurement point is shown in Fig. 13.

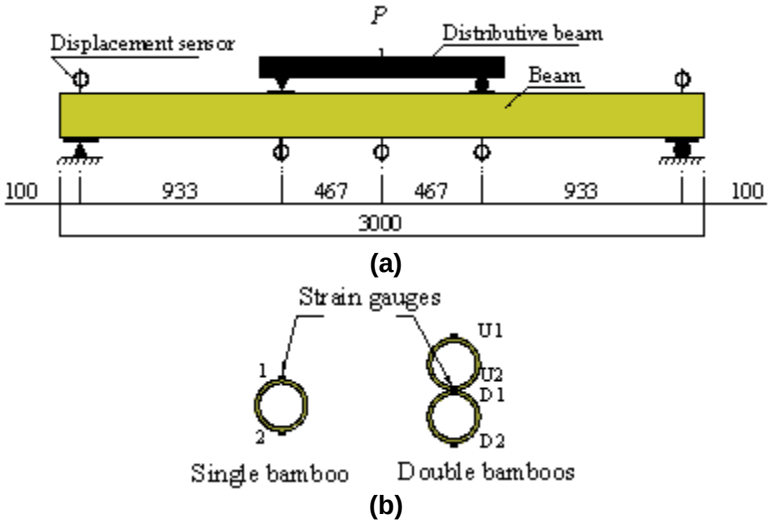

Fig. 13. Locations of the measurement points on the beams: (a) displacement sensors and (b) strain gauges

RESULTS AND DISCUSSION

Diameter Variation of Bamboo

Figure 14 presents the average percentage change for each group of the tests (DV).

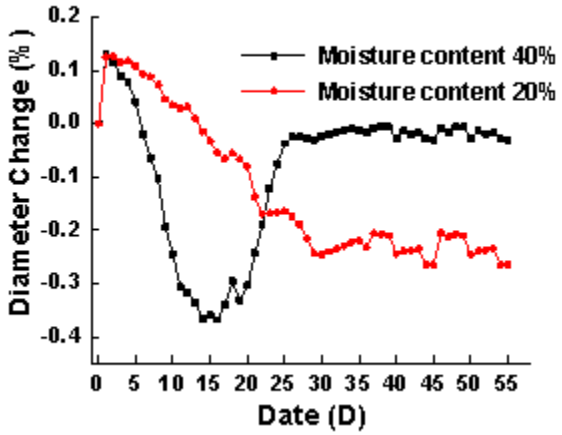

Fig. 14. Change in the bamboo diameter after spraying

After spraying, the diameters of all of the groups (DV) started to increase, and the maximum values were attained after approximately 1 d. Then, the diameters started to shrink. Group S2 shrank five times more rapidly than Group S1.

The diameters of Group S1 continuously decreased during the 30 d following attainment of the maximum value. The amplitude of the change rate variation was 3.9%. In contrast, the diameters of Group S2 decreased and then increased. The amplitude was 4.9%. This showed that the change in the bamboo diameter was more stable at a moisture content of 15% to 25%. The main factors that affected the change in the bamboo diameter were construction factors (spraying); the effects of the ambient temperature and humidity were not obvious.

Thirty days after being sprayed, all of the specimens (DV) underwent gradual changes in the bamboo diameter. During this time, the ambient temperature and humidity had a noticeable impact on the changes in the bamboo diameter. When the temperature increased and the humidity decreased, the bamboo diameters decreased. When the temperature decreased and the humidity increased, the bamboo diameters increased. During this period, the temperature varied from 19.9 °C to 28.3 °C and the humidity varied from 46.9% to 85%. The amplitude of the variation in the change rate was 0.6%. Thus, compared with the spraying construction, the environmental factors had a smaller effect.

Bamboo Moisture Content

After curing, all of the specimens (MC) of Group A became loose and the bamboo and lightweight composite mortar were separated. Groups B and C continued to be loaded. The failure mode of all of the specimens (MC) was push-out destruction (bamboo slipped out of the lightweight composite mortar), with the lightweight composite mortar still intact.

At the beginning of loading, the load increased rapidly and then suddenly decreased. When loading continued, the load decreased and the displacement increased

until the maximum displacement was measured. A clear slip was observed between the bamboo and lightweight composite mortar, which can be seen in Fig. 15.

Fig. 15. Failure mode of the tests (MC)

Figure 16 displays the load-displacement curves of the specimens (MC) from Groups B and C. The curves increased linearly and rapidly in the early stages, and after reaching their extreme, the load abruptly decreased. At this point, the bond between the bamboo and lightweight composite mortar was destroyed and sliding occurred rapidly.

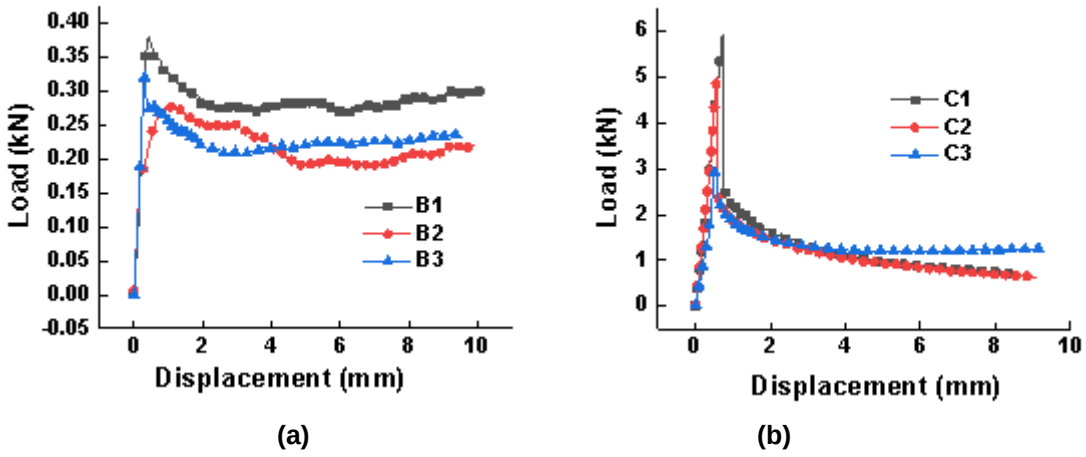

Fig. 16. Load–displacement curves of the specimens from (a) Group B and (b) Group C

The bamboo with a moisture content of 55% to 65% did not bond to the lightweight composite mortar. Figure 16 shows that the ultimate load bearing capacities of Group B were between 250 N and 400 N, whereas those of Group C were between 3000 N and 6000 N. Thus, the bamboo moisture content directly affected the bond performance. A higher bamboo moisture content led to a worse bond performance. This was mainly because of the sharper change in the bamboo size with a higher moisture content during curing after being sprayed. When the moisture content of the bamboo was high (> 65%), spraying was not feasible. Therefore, it was concluded that the moisture content should be kept at 15% to 25% (approximately 20%).

Deflection Behavior and Failure Modes of the Beams

For the original bamboo beams (SBBs and DBBs), the deflection increased gradually with an increase in the load. In the middle compression zone, the beams yielded

when the maximum deflection was close to 60 mm. Then, the load gradually increased and the original bamboo split at the support. The original bamboo beams generally showed a strong deformation ability. The failure modes are displayed in Fig. 17.

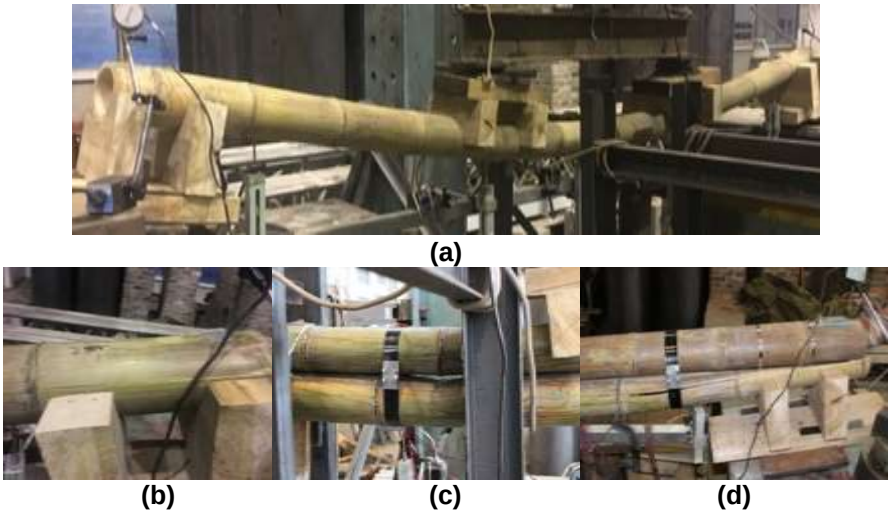

Fig. 17. Failure modes of the original bamboo beams: (a) overall flexure of the SBB; (b) original bamboo in the SBB split at the support; (c) original bamboo in the DBB yielded at the mid-span; and (d) original bamboo in the DBB split at the support

In the case of the composite beams, when the loads of the SCBs and DCBs reached 3 kN and 7 kN, respectively, micro-cracks appeared near the bottom at the mid-span. As loading continued, the load rapidly increased and the cracks widened and extended upward along the side, stopping near the upper side of the original bamboo. Simultaneously, new cracks also appeared. The cracks were concentrated near the mid-span, when the load was close to $0.8P_u$ (where P_u is the ultimate load), for the DCB as an example, as is shown in Figs. 18a and 18b. Finally, the main cracks developed rapidly, and then the specimens were bent at the mid-span (DCB) or loading point (SCB), as is shown in Figs. 18c and 18d.

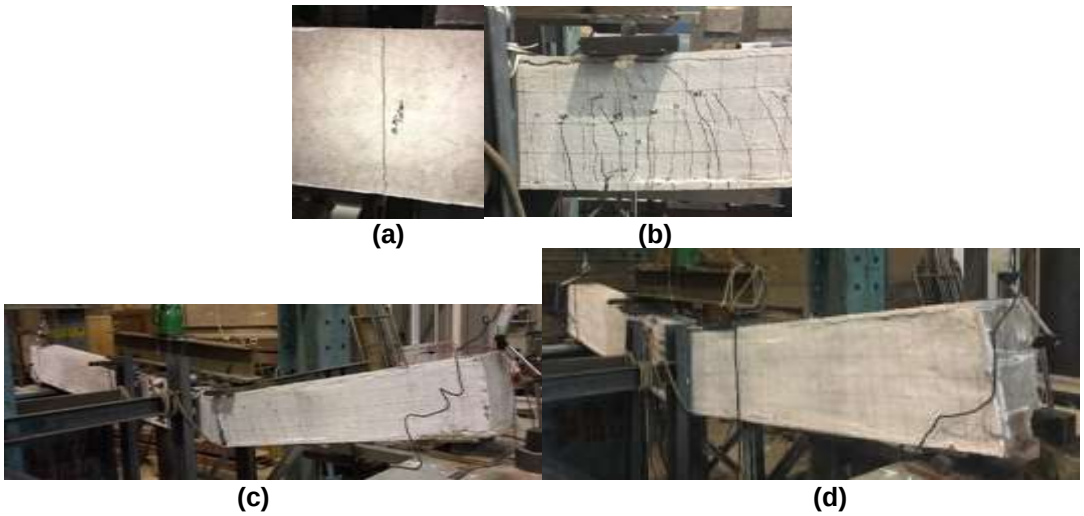

Fig. 18. Failure mode of the composite beams: (a) cracks at the bottom; (b) cracks on the side; (c) SCB; and (d) DCB

Load-displacement curves

The load-deflection curves in the mid-span of the original bamboo beams and composite beams are illustrated in Fig. 19. The curves of the original bamboo beams included three stages. The first was the elastic stage. The load in this stage was approximately 60% of the ultimate load and the curves were linear. Second was the elastoplastic stage. The original bamboo in the middle compression zone yielded and deformation developed rapidly with an increase in the load. The third stage was the failure stage. The original bamboo split at the support and the original bamboo beams did not work. Brittle failure occurred.

The curves of the composite beams can be divided into four stages: the cracking, elastic, elastoplastic, and failure stages. In the cracking stage, the lightweight composite mortar was pulled. In the elastic phase, the overall performance of the composite beams was good, and the combination of bamboo and lightweight composite mortar was effective. In the elastoplastic stage, the lightweight composite mortar gradually cracked, which weakened the effect of the original bamboo combination. The beams flexed rapidly. In the failure stage, at the main crack, the original bamboo split because of the high stress and finally, the composite beams bent.

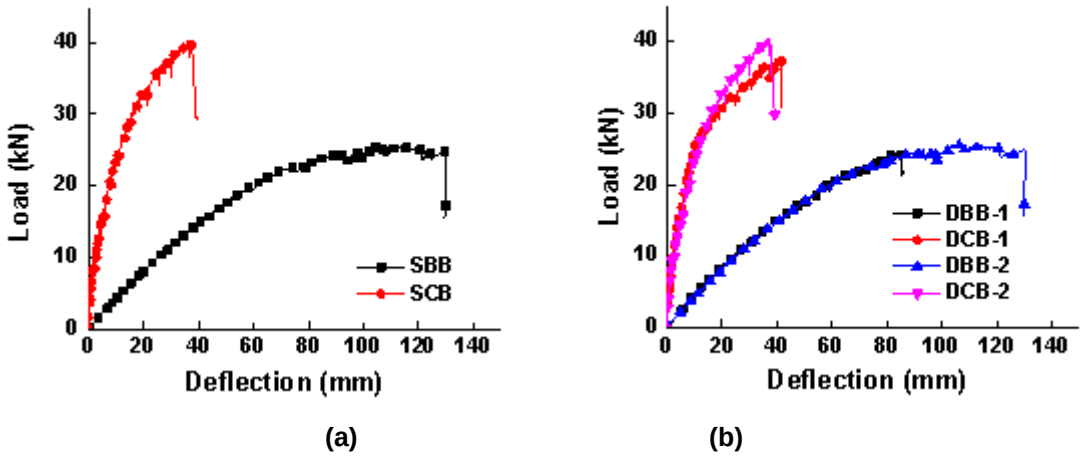

Fig. 19. Load-deflection curves of the beams: (a) SBB and SCB; and (b) DBB and DCB

Load-strain curves

The development of the strain along the upper and lower edges of the original bamboo along the middle load is depicted in Fig. 20. For the original bamboo beam, it was observed that in the first half of the process (load less than $0.6P_u$), the strain varied linearly, and the tensile and compressive strains were nearly symmetrically distributed. In this case, the neutral axis of each original bamboo cross section was near its horizontal axis. The section deformation satisfied the plane assumption. Thereafter, the upper edge compressive strain gradually became larger than the lower edge tensile strain, and the neutral axis was shifted upward. Additionally, the original bamboo beams yielded (when the strain exceeded 5000 με) before the ultimate load was reached. This implied that the strength effect was completely exerted before the original bamboo split.

For the SCB, in the early stage of loading, the upper edge strain of the original bamboo was almost zero, which indicated that the total pressure was applied to the upper lightweight composite mortar and cement mortar.

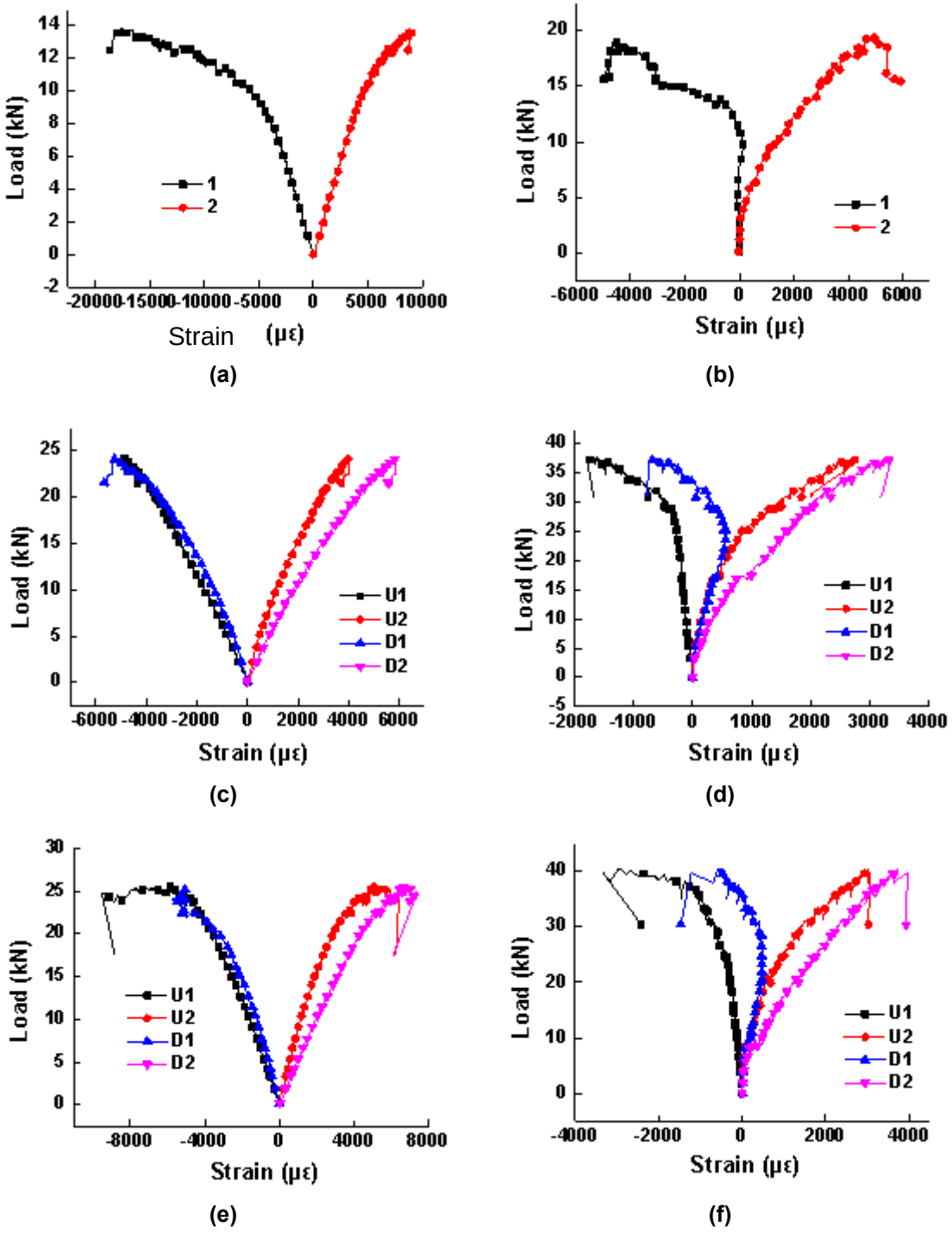

Fig. 20. Load-strain curves of the beams: (a) SBB, (b) SCB, (c) DBB-1, (d) DCB-1, (e) DBB-2, and (f) DCB-2; 1 is the top of the original bamboo cross-section; 2 is the bottom of the original bamboo cross-section; U is the upper original bamboo; and D is the lower original bamboo

As the load increased, the lightweight composite mortar cracked and remained, and the upper part of the original bamboo began to bear the pressure. Regarding the DCB, before reaching the yield load, the top of the upper original bamboo was compressed, whereas the bottom of the upper bamboo and lower bamboo were stretched. Moreover, the

deformations of the bottom of the upper original bamboo and top of the lower original bamboo were consistent, which indicated that the bond strength of the lightweight composite mortar enabled the two bamboos to be effectively joined.

Flexural rigidity

The mechanical properties of the original bamboo make it easy to bend. It is necessary to study the initial flexural rigidity of the original bamboo beams and composite beams within the elastic limit. The results of the load-displacement curves showed that both the original bamboo beams and composite beams were in the elastic stage before the load reached $0.6P_u$, so the initial stiffness (B_i, N/mm) can be calculated in the range of 20% to 40% of the ultimate load with,

$$B = \frac{\Delta P}{\Delta f} \tag{2}$$

where ΔP is the change in the load and Δf is the change in the deflection corresponding to the load change.

The calculation results are presented in Table 4.

Table 4. Results of the Flexural Rigidity

Item	$0.2P_u$ (kN)	$0.4P_u$ (kN)	$f_{0.2Pu}$ (mm)	$f_{0.4Pu}$ (mm)	B (N/mm)
SBB	2.64	5.3	16.7	33.9	154.65
DBB-1	4.84	9.7	10.3	23.3	373.85
DBB-2	5.12	10.2	12.2	25.5	381.95
SCB	3.88	7.8	3	9.7	585.07
DCB-1	7.38	14.8	1.3	4.7	2182.35
DCB-2	7.86	15.7	1.4	5.1	2118.92

Compared with the above data, it was known that the initial flexural rigidity of the DBBs and SCBs was approximately 2.5 and 3.8 times that of the SBB, respectively, in the elastic limit. The initial bending stiffness of the DCB was 5.7 times that of the DBB. The combination effect of the bamboo and lightweight composite mortar was obvious.

Bearing capacity

According to EN 1995-1-1 (2004) and GB 50005-2003 (2003), the deflection limit of the flexural member (beam and grille) is $l_0/250$. Table 5 presents the load when the deflection reaches $l_0/250$ (11.2 mm) and the ultimate load bearing capacity of all of the beams.

Table 5. Bending Capacity

Item	$P_{l0/250}$ (kN)	P_u (kN)	$P_{l0/250}/P_u$ (%)
SBB	2.5	13.2	18.9
DBB-1	5.2	24.2	21.5
DBB-2	5.4	25.6	21.1
SCB	9.5	19.4	48.9
DCB-1	25.6	36.9	69.4
DCB-2	25.7	39.3	65.4

The load of the original bamboo beams in the serviceability limit state was only 20% of the ultimate load bearing capacity, but that of the composite beams was 65% to 75%. This indicated that the composite beams utilized the strength of the lightweight composite mortar. However, the original bamboo beams and composite beams exceeded the serviceability limit state before reaching the ultimate load bearing capacity. Therefore, their design loads should be determined according to the flexural rigidity. Also, the ultimate load bearing capacity of the DBB was twice that of the SCB. The ultimate load bearing capacity of the composite beams was approximately 50% higher than that of the original bamboo beams.

CONCLUSIONS

1. After the lightweight composite mortar was sprayed, the diameters of the bamboo began to increase. They reached their peaks in approximately 1 d and then narrowed and became stable approximately 30 d later. The diameter decrease rate of the bamboo with a moisture content of 40% was approximately five times that of the bamboo with a moisture content of 20%, and the diameters of the bamboo in the two groups tended to become stable after 25 d.
2. A higher moisture content in the bamboo degraded the anti-slip property of the bond interface between the lightweight composite mortar and bamboo. The two components were directly separated when the moisture content was 55% to 65%, and the anti-slip ultimate load bearing capacity reached a maximum when the moisture content was 15% to 25%. Thus, it was concluded that the bamboo moisture content should be kept at approximately 20% before lightweight composite mortar is sprayed.
3. The bamboo of the original bamboo beams and composite beams split at the support and loading points, respectively.
4. The initial flexural rigidity and load bearing capacity of the DBBs were approximately 2.5 times and twice that of the SBBs, respectively. The initial flexural rigidities of the SCBs and DCBs were approximately 3.8 and 5.7 times that of the SBBs and DBBs, respectively. The ultimate load bearing capacity of the composite beams was approximately 1.5 times that of the original bamboo beams. This showed that the lightweight composite mortar had a remarkable strengthening effect on the flexural behavior of the original bamboo.

ACKNOWLEDGMENTS

This research was supported by the National Key Research and Development Program of China (Grant No. 2017YFC0703502), the National Natural Science Foundation of China (Grant No. 51608433), the Science and Technology Co-ordination and Innovation Fund Project of Shaanxi Province of China (Grant No. 2016KTZDSF04-02-02), and the Shaanxi Province Youth Science and Technology New Star Program (2018KJXX-20). The financial support is greatly appreciated.

REFERENCES CITED

Askarinejad, S., Kotowski, P., Shalchy, F., and Rahbar, N. (2015). "Effects of humidity on shear behavior of bamboo," *Theor. Appl. Mech. Lett.* 5(6), 236-243. DOI: 10.1016/j.taml.2015.11.007

Chen, H., Cheng, H., Wang, G., Yu, Z., and Shi, S. Q. (2015). "Tensile properties of bamboo in different sizes," *J. Wood Sci.* 61(6), 552-561. DOI: 10.1007/s10086-015-1511-x

Chung, K. F., and Yu, W. K. (2002). "Mechanical properties of structural bamboo for bamboo scaffoldings," *Eng. Struct.* 24(4), 429-442. DOI: 10.1016/s0141-0296(01)00110-9

Dixon, P. G., Ahvenainen, P., Aijazi A. N., Chen, S. H., Lin, S., Augusciak, P. K., Borrega, M., Svedström, K., and Gibson, L. J. (2015). "Comparison of the structure and flexural properties of moso, guadua and tre gai bamboo," *Constr. Build. Mater.* 90, 11-17. DOI: 10.1016/j.conbuildmat.2015.04.042

Dixon, P. G., and Gibson, L. J. (2014). "The structure and mechanics of moso bamboo material," *J. R. Soc. Interface* 11(99). DOI: 10.1098/rsif.2014.0321

EN 1995-1-1 (2004). "Eurocode 5: Design of timber structures – Part 1-1: General – Common rules and rules for buildings," European Committee for Standardization, Brussels, Belgium.

GB 50005-2003 (2003). "Code for design of timber structures," Standardization Administration of China, Beijing, China.

Huang, Z., Chen, Z., Huang, D., and Zhou, A. (2016). "The ultimate load-carrying capacity and deformation of laminated bamboo hollow decks: Experimental investigation and inelastic analysis," *Constr. Build. Mater.* 117, 190-197. DOI: 10.1016/j.conbuildmat.2016.04.115

ISO 22157-1:2004 (2004). "Bamboo - Determination of physical and mechanical properties–Part 1: Requirements," International Organization for Standardization, Geneva, Switzerland.

Kaminski, S. (2013). "Engineered bamboo houses for low-income communities in Latin America," *Struct. Eng.* 91(10), 14-23.

Li, H.-t., Chen, G., Zhang, Q., Ashraf, M., Xu, B., and Li, Y. (2016). "Mechanical properties of laminated bamboo lumber column under radial eccentric compression," *Constr. Build. Mater.* 121, 644-652. DOI: 10.1016/j.conbuildmat.2016.06.031

Liu, B., Hao, J.-P., Zhong, W.-H., and Wang, H. (2016). "Performance of cold-formed-steel-framed shear walls sprayed with lightweight mortar under reversed cyclic loading," *Thin Wall. Struct.* 98(Part B), 312-331. DOI: 10.1016/j.tws.2015.09.024

Lo, T. Y., Cui, H. Z., and Leung, H. C. (2004) "The effect of fiber density on strength capacity of bamboo," *Mater. Lett.* 58(21), 2595-2598. DOI: 10.1016/s0167-577x(04)00214-9

Nurdiah, E. A. (2016). "The potential of bamboo as building material in organic shaped buildings," *Procd. Soc. Behv.* 216, 30-38. DOI: 10.1016/j.sbspro.2015.12.004

Nurmadina, Nugroho, N., and Bahtiar, E. T. (2017). "Structural grading of *Gigantochloa apus* bamboo based on its flexural properties," *Constr. Build. Mater.* 157, 1173-1189. DOI: 10.1016/j.conbuildmat.2017.09.170

Ray, A. K., Mondal, S., Das, S. K., and Ramachandrarao, P. (2005). "Bamboo - A functionally graded composite-correlation between microstructure and mechanical strength," *J. Mater. Sci.* 40(19), 5249-5253. DOI: 10.1007/s10853-005-4419-9

Sharma, B., Gatoo, A., Bock, M., Mulligan, H., and Ramage, M. (2015). "Engineered bamboo: State of the art," *P. I. Civil Eng.* 168(2), 57-67. DOI: 10.1680/coma.14.00020

Sinha, A., Way, D., and Mlasko, S. (2014). "Structural performance of glued laminated bamboo beams," *J. Struct. Eng.* 140(1), 896-912. DOI: 10.1061/(asce)st.1943-541x.0000807

Tan, T., Rahbar, N., Allameh, S. M., Kwofie, S., Dissmore, D., Ghavami, K., and Soboyejo, W. O. (2011). "Mechanical properties of functionally graded hierarchical bamboo structures," *Acta Biomater.* 7(10), 3796-3803. DOI: 10.1016/j.actbio.2011.06.008

Tian, L. M., Hao, J. P., Kou, Y. F., Xu, K., and Zhao, Q. L. (2018). "Experimental study on bond-slip behavior of bamboo-thermal insulation material interface," *J. Build. Mater.* 21(1), 65-70. DOI: 10.3969/j.issn.1007-9629.2018.01.011

van der Lugt, P., van den Dobbelsteen, A. A. J. F., and Janssen, J. J. A. (2006). "An environmental, economic and practical assessment of bamboo as a building material for supporting structures," *Constr. Build. Mater.* 20(9), 648-656. DOI: 10.1016/j.conbuildmat.2005.02.023

Wei, Y., Ji, X., Duan, M., and Li, G. (2017). "Flexural performance of bamboo scrimber beams strengthened with fiber-reinforced polymer," *Constr. Build. Mater.* 142, 66-82. DOI: 10.1016/j.conbuildmat.2017.03.054

Xiao, Y., Yang, R. Z., and Shan, B. (2013). "Production, environmental impact and mechanical properties of glubam," *Constr. Build. Mater.* 44, 765-773. DOI: 10.1016/j.conbuildmat.2013.03.087

Yang, X., Tian, G., Shang, L., Lv, H., Yang, S., and Liu, X. (2014). "Variation in the cell wall mechanical properties of *Dendrocalamus farinosus* bamboo by nanoindentation," *BioResources* 9(2), 2289-2298. DOI: 10.15376/biores.9.2.2289-2298

Article submitted: August 20, 2018; Peer review completed: October 20, 2018; Revised version received: October 24, 2018; Accepted: November 22, 2018; Published: November 28, 2018.
DOI: 10.15376/biores.14.1.500-517